International Journal of Technology 14(2) 276-289 (2023)
Received August 2021 / Revised September 2021 / Accepted November 2021

International Journal of Technology

Nickel Supported on MIL-96(Al) as an Efficient Catalyst for Biodiesel and Green Diesel Production from Crude Palm Oil

Afifah Nur Aisyah[1], Dwi Ni'maturrohmah[1,2], Riandy Putra[1,3], Syaiful Ichsan[1], Grandprix T. M. Kadja[4,5,6], Witri Wahyu Lestari[1*]

[1]*Chemistry Department, Faculty of Mathematics and Natural Sciences, Universitas Sebelas Maret, Jl. Ir. Sutami No.36A, Kentingan, Jebres-Surakarta, Central Java, 57126, Indonesia*
[2]*Research Center for Food Technology and Processing (PRTPP), National Research and Innovation Agency (BRIN), Gunungkidul, Yogyakarta 55861, Indonesia*
[3]*Department of Chemistry, Faculty of Mathematics and Natural Sciences, Universitas Palangka Raya, Kampus UPR Tunjung Nyaho, Palangka Raya, Indonesia*
[4]*Division of Inorganic and Physical Chemistry, Faculty of Mathematics and Natural Sciences, Institut Teknologi Bandung, Jalan Ganesha No. 10, Bandung 40132, Indonesia*
[5]*Center for Catalysis and Reaction Engineering, Institut Teknologi Bandung, Jalan Ganesha No. 10, Bandung 40132, Indonesia*
[6]*Research Center for Nanosciences and Nanotechnology, Institut Teknologi Bandung, Jalan Ganesha No. 10, Bandung 40132, Indonesia*

Abstract. In this study, a new class of heterogeneous catalyst in the form of metal-organic frameworks (MOFs), namely Material of Institute Lavoisier-96(Al), which is called MIL-96(Al), was employed for the production of biodiesel and green diesel. The synthesis of MIL-96(Al) was conducted *via* a hydrothermal method at 210 °C for 4 hours with dimethylformamide (DMF) as an assisting agent. The Ni was loaded into MIL-96(Al) *via* incipient wetness impregnation method with variations 3, 5, and 10 wt.% to form Ni/MIL-96(Al). Based on X-Ray diffraction (XRD) analysis, the obtained material has good crystallinity with characteristic peaks observed at 2θ = 5.8°; 7.8°, and 9.1°. Fourier Transform Infrared (FTIR) analysis demonstrated an essential shift from 1715 cm^{-1} to 1666 $cm^{-1,}$ indicating the coordination of the carboxylate group with Al^{3+} metal ions. Moreover, MIL-96(Al) is stable up to 390 °C according to the thermogravimetric analysis (TGA). Based on structural and morphological analysis (using XRD, FTIR, and Scanning Electron Microscope (SEM)), the loading of Ni into MIL-96(Al) does not change the basic structure of MIL-96(Al). However, the pore diameter of MIL-96(Al) decreased from 5.7 nm to 1.4 nm after the Ni was embedded in the structure. The largest surface area was obtained from 10% Ni/MIL-96(Al) (up to 595.5 m^2/g). The catalytic test exhibits that 3% Ni/MIL-96(Al) could attain an optimum yield of up to 85.24% of biodiesel, while in the case of hydrodeoxygenation (HDO) reaction, the optimum catalyst shown by 10% Ni/MIL-96(Al) with conversion and selectivity of C_{16} up to 90.70% and 55.22%, respectively.

Keywords: Biodiesel; Green diesel; Hydrodeoxygenation; Ni/MIL-96(Al); Trans-esterification

1. Introduction

The highlighted impact of the population and industrial sector growth has been significantly increased due to the global energy demand. Based on the United States Energy

*Corresponding author's email: witri@mipa.uns.ac.id, Tel.: +62 (0271) 669376
doi: 10.14716/ijtech.v14i2.5064

Information Administration (U.S. EIA) International Energy Outlook 2017, the total energy requirement is predicted to increase up to 28% from 2015 to 2040 (Capuano, 2020). Meanwhile, reserves and the production of fossil fuels are threatened to be limited. Moreover, the use of fossil fuels as the main energy source causes scarcity and air pollution. Therefore, changing fossil-based energy to environmentally friendly renewable energy is necessary. Biomass feedstocks (either lignocellulose or triglyceride) have been proposed and widely studied as sustainable resources for generating of renewable fuels. Several review articles have discussed comprehensive information on this matter (Hoang *et al.*, 2021a-c; Zhao *et al.*, 2017). One of the potential alternative energies to be developed in Indonesia is palm oil-based biofuels, like biodiesel and green diesel.

Biodiesel can be produced through a trans-esterification reaction, while green diesel (the 2nd generation of diesel) is manufactured through an HDO reaction (Prihadiyono *et al.*, 2022; Muharam and Adinda, 2018; Putra *et al.*, 2018; Susanto *et al.*, 2016). Hoang and Li (2019) thoroughly examined biodiesel as a fuel in diesel engines, focusing on engine performance, deposit formation, combustion, and emissions characteristics. In addition, biodiesel manufacturing employing various processes and catalysts (e.g., heterogeneous catalysts) has also been extensively described in multiple review articles (Cong *et al.*, 2021; Hoang *et al.*, 2021). Heterogeneous catalysts have been studied and significantly impacted the reaction stage. In addition, heterogeneous catalysts are greener due to the ease of handling and separation from the product and reusability. One relatively new class of promising materials for the heterogeneous catalyst is Metal-Organic Frameworks (MOF) (Yap, Fow, and Chen, 2017; Xamena and Gascon, 2013).

MOFs are organic-inorganic hybrid nanoporous materials consisting of metal cations or metal oxide clusters as nodes and bidentate or poli-dentate ligands as organic linkers to form infinite networks. MOFs combine the advantages of homogeneous and heterogeneous catalysts due to their unique features such as nanoporosity, thermal and chemical stability, insolubility in water and organic solvents, and the presence of various catalytic active sites. The catalytic activity of MOFs depends on their active site, which can be derived from unsaturated metal centers, functionalized organic linkers, as well as additional metal sites inserted *via* post-synthesis modification (Huang *et al.*, 2017). As a catalyst, MOFs should have a stable porosity that can be accessed by the substrates.

Material of Institut Lavoisier-96(Al) [MIL-96(Al)] represents the first synthesized MOFs using Al^{3+} metal ions as nodes and trimesic acid [benzene-1,3,5-tricarboxylic] or H_3BTC as ligand by hydrothermal method resulting $[Al_{12}O(OH)_{18}(H_2O)_3(Al_2(OH)_4)[BTC]_6 4H_2O$ (Loiseau *et al.*, 2006). MIL-96(Al) is stable up to 500 °C and has a high BET surface area (*ca.* 687 m^2/g) as well as an average pore radius and total pore volume of 0.97 nm and 0.335 cc/g, respectively (Abid *et al.*, 2016). The use of Al^{3+} as a trivalent metal ion node causes higher thermal and chemical stability than divalent metal ions (Chughtai *et al.*, 2015). MIL-96(Al) was first synthesized *via* the hydrothermal method employed by Loiseau *et al.* (2006) for 24 hours at 210 °C. Yang *et al.* (2016) innovated to use of assisting agents such as methanol, ethanol, diethylformamide (DEF) or dimethylformamide (DMF) in the synthesis of MIL-100(Al) with a shorter time of only for 4 hours at 210 °C. Moreover, the advantage of using DMF as an assisting agent is that it could produce material with better crystallinity.

Several MOFs were tested as heterogeneous catalysts in esterification and trans-esterification reactions such as HSO_3-MIL-101(Cr) and HSO_3-(Zr) MOF (Juan-Alcañiz *et al.*, 2013), ZIF-8 (Chizallet *et al.*, 2010) and $[HPW/Cu_3(BTC)_2]$ (Wee *et al.*, 2011). Peng *et al.* (2012) conducted metal impregnation and found that Ni metal loaded into zirconium oxide increases catalytic activity in the selective reduction of microalgae oil into alkanes resulting

in high selectivity for C_{17} (up to 96%). Nickel in the form of metal nanoparticles has also been incorporated into MOF-5 (Zhao, Chou, and Song, 2012) and Zn-MOCP (Zhao Chou, and Song, 2011) through wet impregnation. These materials have been used for hydrogenation reactions of crotonaldehyde, as well as for improving catalytic activity and stability in CO_2 methanation (Zhen *et al.*, 2015). Furthermore, Ni metal exposure in MIL-120(Al) also has shown activity prominently converting 100% of benzene to cyclohexane in hydrogenation reaction as reported by Wan *et al.* (2013).

Considering biofuel sustainability, Fang *et al.* (2020) reviewed the use of metal-organic frameworks (MOFs) and derivatives as catalysts for biomass conversion, including lignocellulosic feedstocks. Previous research conducted by Čelič *et al.* (2015) reported that 3wt.% Ni/MIL-77 catalyst showed high hydrogenolysis activity during hydrotreatment of biomass material (lignocellulose) and successfully converted biomass oil into polar and non-polar phases. Noteworthily, MOF-derived catalyst on the valorization of lignocellulosic demonstrated the synergism between active sites and functionalized ligands for enhancing the catalytic activity (Liao, Matsagar, and Wu 2018). Hence, remarkable attention has been devoted to the development of innovative MOF catalysts for value-added biochemical production (Khemthong *et al.*, 2021). MIL-96(Al) and its post-synthesis with Ni metal, which could perform as a heterogeneous catalyst for transesterification processes and hydrogenation, have never been studied before. This research will present an innovative synthetic method of MIL-96(Al) in the presence of DMF as an assisting agent. Furthermore, the material was then embedded with nickel in various weight percent (3, 5, and 10 wt.%) and tested as a catalyst in esterification-transesterification and hydrogenation as well as HDO reaction of CPO forming biodiesel and green diesel.

2. Methods

2.1. Materials

All chemicals used in this research are in analytical grade and used as received without further purification. Aluminum nitrate nonahydrate, $Al(NO_3)_3{\cdot}9H_2O$ (98%), and benzene-1,3,5-tricarboxylic acid (H_3BTC) (95%) were purchased from Sigma Aldrich, Germany. Nickel(II) nitrate hexahydrate, $Ni(NO_3)_2{\cdot}6H_2O$ (98%), nitric acid (HNO_3), N-N′ dimethyl formamide (DMF, 99.8%), ethanol (96%), and methanol (96%) were commercially obtained from Merck, Germany. Crude Palm Oil (CPO) was obtained from PT. Salim Ivomas Pratama Tbk., nitrogen, and hydrogen gas (UHP, 99,9%) was supplied by PT. Samator Indonesia. Other materials, such as pH paper, filter paper, acetone, and aquadest, were obtained from Bratachem Indonesia.

2.2. Synthesis of MIL-96(Al)

The synthesis of MIL-96(Al) was performed *via* a hydrothermal method based on modified and combined previous procedures reported by Loiseau *et al.* (2006) and Yang *et al.* (2016). $Al(NO_3)_3{\cdot}9H_2O$ (0.75 g, 2.40 mmol) and H_3BTC (0.35 g, 1.67 mmol) were dissolved in 10 mL of aquadest. Subsequently, 0.2 mL DMF was added slowly then stirred for 10 minutes to form a homogeneous solution. HNO_3 (4M) was added dropwise to the solution until pH 1. The solution was then placed into Teflon vessels covered with stainless-steel autoclaves and heated at 210 °C for 4 hours. The final product was filtered and washed with ethanol to remove the residual acid. The yellow precipitate was dried at room temperature and activated at 200 °C for 2 hours.

2.3. Loading Ni into MIL-96(Al)

Loading of nickel into MIL-96(Al) was conducted through the incipient wetness impregnation method refers to previous procedures reported by Peng *et al.* (2012).

$Ni(NO_3)_2 \cdot 6H_2O$ metal salts as Ni source was loaded into MIL-96(Al) with variation 3, 5, and 10 wt.% of 2 g of MIL-96(Al). The mixture of $Ni(NO_3)_2 \cdot 6H_2O$ and MIL-96(Al) was stirred in 10 mL of aquadest at room temperature for 24 hours, then filtered, dried and calcined, and reduced at 200 °C for 2 h under nitrogen and hydrogen atmosphere (with a 15 mL/min flow rate) (Figure 1).

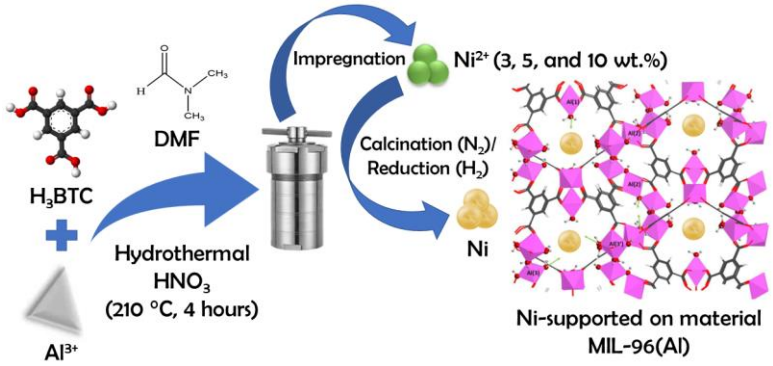

Figure 1 Schematic illustration showing the preparation of Ni/MIL-96(Al) catalyst

2.4. Materials Characterization

X-ray diffraction (XRD) measurements were carried out on a Rigaku Miniflex 600 Benchtop (Cu-Kα beam with λ = 1.5406 Å) in 2θ range of 5-50˚. SEM type: inspect S50-FEI equipped with EDX analysis was used to analyze the morphology of materials and its elemental composition. FTIR spectroscopy type Shimadzu IR Prestige-21 in KBr pellets was used to analyze the change in the functional group of the material and recorded in the wavenumber range of 400-4000 cm^{-1}. A Quadrasorp evo (Quantachrome instruments) was used to measure nitrogen sorption isotherm at 77 K. Thermal stability of the materials was investigated using STA Linseis PT-1600 from 30 until 700 °C under nitrogen flow with a heating rate of 20 °C/min.

2.5. Catalytic test of MIL-96(Al) and Ni/MIL-96(Al)

The catalytic activity in the transesterification reaction of CPO into biodiesel was carried out in a batch system by mixing the catalyst material, CPO:methanol (1:4 of volume), and heating at 60 °C for 5 h. The final product was extracted using a separation funnel until it formed two phases, biodiesel, and glycerol. The upper phase (biodiesel) was analyzed using GC-MS. The HDO reaction of CPO was carried in an autoclave hydrotreating batch reactor with a feed ratio of 50 mL:0.5 g (CPO:catalyst), equipped with a stirrer, condenser and pump, as shown in Figure 2. The HDO reactions were performed at 200 °C with 10 bar of H_2 pressure for 2 hours. The bottom product was distilled using a Koehler Model K 45090 with the American Society for Testing and Materials (ASTM)-D86 method. A gas chromatography-mass spectroscopy (GC-MS) (Agilent Technologies 7890A gas chromatograph (HP-INNOWax with capillary column 30 m × 0.25 mm × 0.20 µm film thickness) with an autosampler and a 5975C mass selective detector) was used to analyze the HDO products. The measurements started at 40 °C for 0.5 minutes, increased at 8 °C/min to 195 °C in 0 minutes, and finally increased at 1 °C/min to 225 °C and held for 22 minutes. Helium carrier gas (1.8614 mL/min) was used, and an injection volume of 1 µl was used to identify the HDO product components. The formula defined by Equation (1) was used to calculate the biodiesel conversion (Carmo *et al.*, 2009):

$$\% \text{ Conversion} = \frac{a_i - a_f}{a_i} \times 100 \quad (1)$$

Where a_i is the initial fatty acid of the mixture, and a_f is the fatty acid in the final mixture. The conversion and selectivity of HDO products were defined using Equation (2) and (3), according to Putra *et al.* (2018):

$$C = 100\% - C_{(TG)} \quad (2)$$

$$S = \frac{Y_i}{C} \times 100\% \quad (3)$$

Where $C_{(TG)}$ represents the triglyceride concentration (%) in the oil product as evaluated by GC, Y_i represents the yield of C_{16} hydrocarbons (%) as determined by GC analysis, and C represents the crude palm oil conversion (%) as determined by the Equation (2).

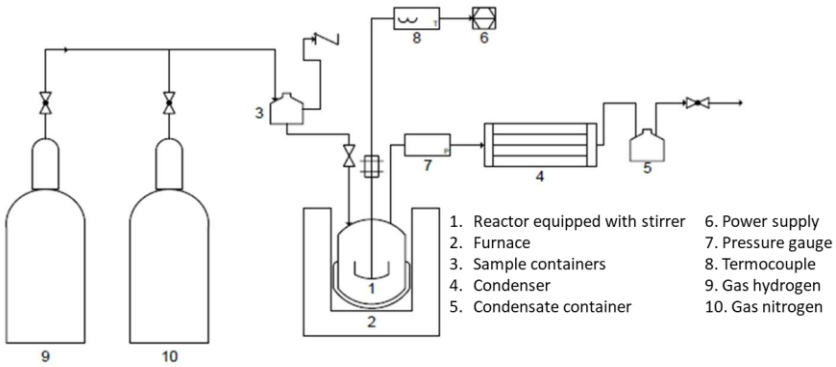

Figure 2 Experiment setup and apparatus of HDO reactor (Putra *et al.*, 2018)

3. Results and Discussion

3.1. Materials Characterization

XRD analysis (Figure 2, left) shows that MIL-96(Al) was successfully synthesized. Three prominent peaks at 2θ: 5.8° (002), 7.8° (101), and 9.1° (102) are confirmed through similarity with the standard pattern of MIL-96(Al) generated from CCDC No. 622598 (Loiseau *et al.*, 2006). DMF utilization as an assisting agent produces MIL-96(Al) in a shorter time with high crystallinity (Yang *et al.*, 2016). However, the peaks identified at 2θ around 11°-27° are observed to be the remaining H_3BTC ligand. Further diffractogram shown in Figure 3 (right) compares MIL-96(Al) and loaded MIL-96(Al) with Ni 3, 5, and 10 wt.%. The peaks found at 2θ: 20.38°, 23.51° and 41.09° indicate the presence of Ni according to JCPDS No. 01-1266. In addition, Ni loading did not alter the basic structure of MIL-96(Al) based on the remaining three main peaks, as discussed before.

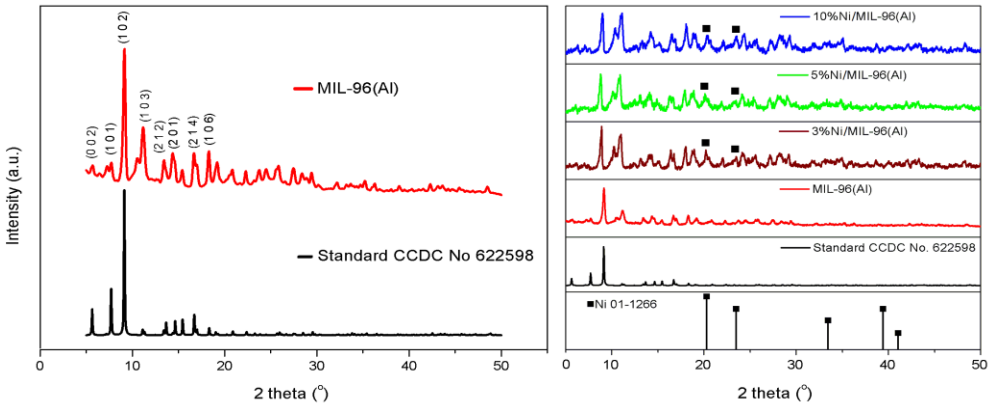

Figure 3 X-Ray Diffractogram of synthesized MIL-96(Al) compared to the simulated pattern (CCDC 622598) (left) and Ni/MIL-96(Al) in comparison with MIL-96(Al) and Ni standard (right)

Corresponding to the FTIR spectra of MIL-96(Al) (Figure 4), the absorption band at 1715 cm^{-1} is defined as the C=O stretching vibration of the carboxylate group in H_3BTC. It shifts significantly to 1665.6 cm^{-1} after C=O coordinated with Al^{3+} in the MIL-96(Al) formation. Moreover, the absorption at 3000-3100 cm^{-1} and 1461 cm^{-1} reveals stretching vibration of C–H and C=C in aromatic groups of BTC parts. Al–O vibration is indicated by the peak at 768-734 cm^{-1}, as reported in a previous study (Liu *et al.*, 2015). Furthermore, the absorption peak shift from 3300-2500 cm^{-1} to 3416 cm^{-1} shows the existence of water coordination on Al^{3+}-BTC and formed hydrogen bonding. Due to the same profile of FTIR spectra before and after loading with nickel (Figure 4, right) confirms that the main functional groups constructing the structure of MIL-96(Al) remained unchanged after Ni loading.

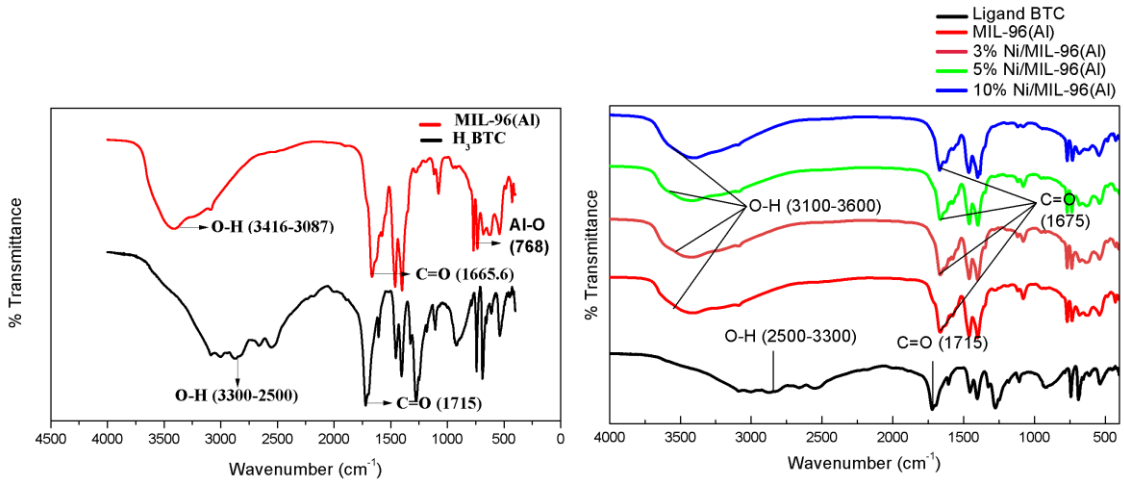

Figure 4 FTIR spectra of MIL-96(Al) in comparison with H_3BTC (left) and MIL-96(Al) compared to Ni/MIL-96(Al) (right)

Figure 5 (left) shows type II N_2 adsorption-desorption isotherm indicating the mixture of micro and mesoporosity in the material. The loading of Ni at 3, 5, and 10 wt.% into MIL-96(Al) results in an increase in surface area and a decrease in pore volume, as shown in Table 1. Therefore, it may be assumed that Ni impregnation successfully filled the pores of MIL-96(Al). Furthermore, the Brunner-Emmett-Teller (BJH) pore distribution revealed that the pore volume distribution of the materials changed to have an inhomogeneous size after being loaded with Ni (Figure 5, right). However, the materials still fall within the range of micro- and mesoporous materials.

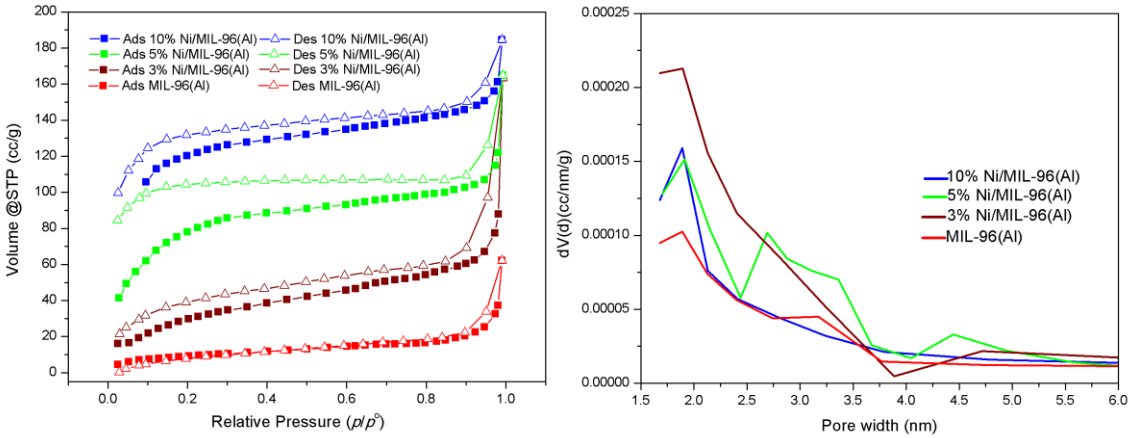

Figure 5 Nitrogen adsorption-desorption isotherm (left) and BJH pore size distribution (right) of MIL-96(Al) and Ni/MIL-96(Al) (right)

Table 1 Textural properties of MIL-96(Al) and various Ni/MIL-96(Al)

Material	Surface Area (m^2/g)	Pore size (nm)
MIL-96(Al)	52.93	5.70
3% Ni/MIL-96(Al)	191.3	4.43
5% Ni/MIL-96(Al)	432.3	1.84
10% Ni/MIL-96(Al)	595.5	1.43

SEM images (Figure 6) describe that the morphology of MIL-96(Al) is hexagonal with an average particle size in the range of 0.5-1.5 µm in accordance with previous studies (Liu *et al.*, 2015; Peng *et al.*, 2012). In addition, this result suggests that Ni metal exposure does not damage the morphology of MIL-96(Al) and is well distributed on the surface and pore of the host materials. SEM-EDX analysis (Table 2) showed that Ni nanoparticle was successfully embedded into MIL-96(Al). However, the weight of Ni particles was not exactly detected based on theoretical calculation. The low amount of Ni metals is caused by several factors, such as a long process prior to analysis, then Ni metals might be partially lost during the filtration stage, drainage, or reduction process.

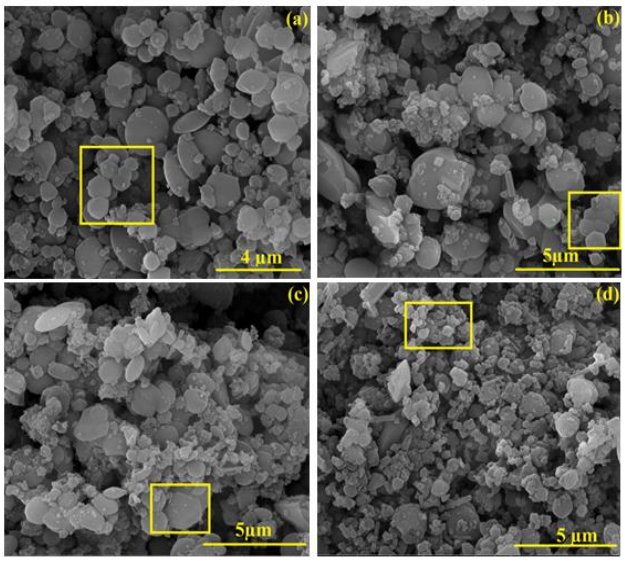

Figure 6 SEM images of (a) MIL-96(Al); (b) 3% Ni/MIL-96(Al); (c) 5% Ni/MIL-96(Al) and (d) 10% Ni/MIL-96(Al) with magnification 20kx

Table 2 Elemental Composition of MIL-96(Al) and Ni/MIL-96(Al) determined by EDX

Material	Elemental composition (wt.%)			
	Ni	C	O	Al
MIL-96(Al)	-	37.73	40.73	21.54
3% Ni/MIL-96(Al)	1.09	41.06	40.18	17.68
5% Ni/MIL-96(Al)	1.66	40.09	41.5	16.75
10% Ni/MIL-96(Al)	6.55	38.85	33.72	20.89

The thermal stability of MIL-96(Al) (presented in Figure 7, left) was studied by thermogravimetric analysis. It can be explained by two different regions of mass loss. The first weight loss of 26.95% occurred between 34 °C and 200 °C indicating the removal of 42 molecules of H_2O as the solvent, which is estimated 39 molecules of H_2O are on the surface and trapped in pores and 3 other H_2O molecules coordinate with metal ions Al^{3+} on MIL-96(Al). A sudden weight loss of 52.53% at the second period from 391 to 598 °C is the degradation of MIL-96(Al) structure, as confirmed in the previous literature studies (Liu *et*

al., 2015; Loiseau *et al.*, 2006). After that, the thermogram did not show any change up to 644 °C, and the weight remained at 20.52%, which is expected as the Al_2O_3 phase as reported by Loiseau *et al.* (2006) Ni loaded into MIL-96(Al) did not change the thermal stability of MIL-96(Al) as shown in Figure 7 (right).

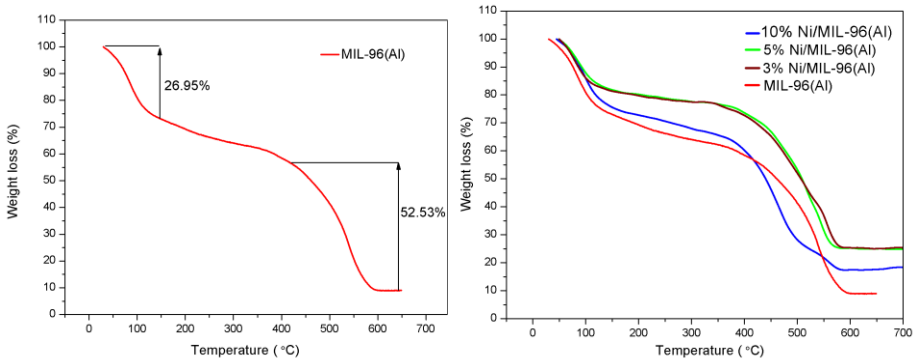

Figure 7 TGA curve of MIL-96(Al) (left) and Ni/MIL-96(Al) in comparison with MIL-96(Al) (right)

3.2. Catalytic Test

As a preliminary study, a catalytic activity test of MIL-96(Al) and Ni/MIL-96(Al) was performed to convert CPO into biodiesel through a trans-esterification reaction. Figure 8 shows catalytic activity increased after Ni metal was loaded into MIL-96(Al). Loading of Ni 3 wt.% resulted in a significant change of up to 85.2% of yield compared to unloaded MIL-96(Al), which converted only 51.8%. However, loading 5 and 10 wt.% Ni only achieved the conversion up to 55.4% and 61.4%, respectively. Therefore, 3% Ni/MIL-96(Al) was selected as the optimum catalyst in this reaction due to the occupancy of suitable pore size between the host catalytic material and the substrate size. In our earlier investigations, Larasati *et al.* (2017) discovered that employing Zr^{4+}-BTC based MOF with 0.6 wt.% catalyst results in a maximum conversion of biodiesel of 69.2%. Furthermore, Ni/MIL-96(Al) serves as a bimetallic catalyst with a stronger active site and higher Lewis acid catalyst properties than MIL-96(Al). Finally, it leads to better catalytic performance and greater product conversion.

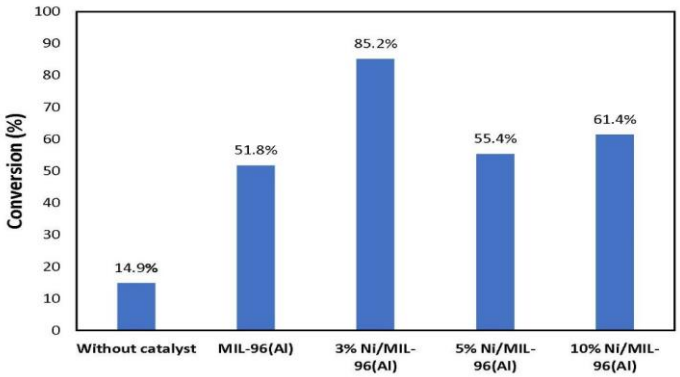

Figure 8 The graph of the conversion result of CPO into biodiesel with MIL-96(Al) and Ni/MIL-96(Al) as catalyst and without catalyst

As an innovation, the HDO reaction of CPO has also been investigated over the prepared MIL-96(Al) and Ni embedded into MIL-96(Al) with different Ni contents at 200 °C under pressure 10 bar H_2 for 2 hours. Figure 9 and Table 3 show the catalytic test results and liquid phase product distribution of HDO reaction over CPO using MIL-96(Al) and its

variation with Ni metals as the catalyst. The observed main product is hydrocarbon diesel fraction generally consisting of a straight chain of *n*-paraffin (C_{10}-C_{17}), with low amounts of by-products such as light alkanes and kerosene which involve the oxygenates, alkenes and aromatics as the intermediates. Meanwhile, as reported previously, CO_2, CO, CH_4, and propane could also serve as gas products (Putra *et al.*, 2022; Muharam and Sudarsono, 2020; Putra *et al.*, 2018; Peng *et al.*, 2012).

MIL-96(Al) reached 5.83% of yield C_{15} alkane, while Ni 5 wt.% increased this product up to 7.01% compared to pristine MIL-96(Al) (Figure 9). This reaction is supposed to take place *via* the decarbonylation/decarboxylation mechanism of CPO (consisting of palmitic acid) with CO/CO_2 as the by-products as proposed by Zuo *et al.* (2012). Research conducted by Hachemi et al. (2017) has proven that the metallic Ni strongly promotes decarbonylation and/or decarboxylation in the ester hydrogenation reaction. In addition, the proportion of loaded Ni determines the level of catalytic performance.

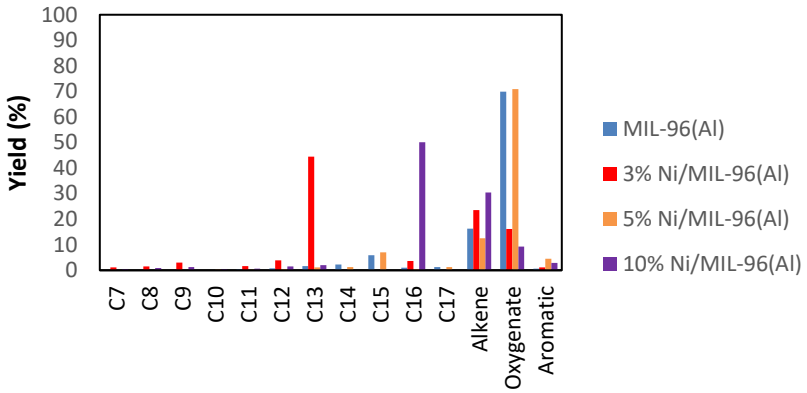

Figure 9 Catalytic test results of MIL-96(Al) and Ni/MIL-96(Al) in HDO reaction of CPO

Loading of 10 wt.% Ni achieved HDO product from CPO up to 50.09% of yield C_{16} alkane (Table 3). The production of C_{16} hydrocarbons with the selectivity 55.22% promoted hydrogenolysis of C–O by the interaction of Lewis acid from metallic Ni and oxygen atom (CPO) produced low oxygenated with H_2O as a side product. In comparison to our previously published MOF-based catalysts by Lestari *et al.* (2021), palladium supported MIL-100(Fe) as a selective catalyst in the hydrogenation of citronellal showed a selectivity of 22.2% of citronellol products. Thus, in view of their remarkable designability, replacing palladium metals in heterogeneous hydrogenation catalysts with low-cost metals (e.g. nickel) for the creation of Ni–H bonds (nickel hydride bonds) has driven scientists as a desirable novel class of catalytic materials.

The presence of Ni catalyst promotes the adsorption of substrates (reactants) more effectively, thus facilitating the electron transfer from Ni's *d*-orbital to bond the hydrogen's orbital (Chen *et al.*, 2018). Some unfilled energy levels in the *d*-orbital of nickel will form lone pair electrons and can form chemical bonding with the adsorbed substrates. Hydrogen molecules are then activated and broken down from "H–H" bonds to generate "Ni-H" through a spillover mechanism, generating highly reactive dissociative hydrogen species that are essential for catalytic hydrogenation reactions (Figure 10). Palmitic acid is the most important component of CPO in this study (40.77 wt.%). The presence of Ni predominantly speeds up the hydrodeoxygenation reaction in this research, which agrees with another group's study (Chen *et al.*, 2018; Zuo *et al.*, 2012). Direct C–O bonds scission with the release H_2O as a by-product (direct HDO) is the suggested mechanism for carboxylic acid hydrogenation, which results in *n*-C_{16} alkanes (without carbon loss) (Figure 10). The C=O double bond is initially cleaved during direct HDO, leading to the production of alcohol. In

addition, the C–O bond is hydrogenated, resulting in alkane formation. Nickel has been shown to be an active component in the C=O and C–O breakings in palmitic acid hydrodeoxygenation. Generally, the distribution of desirable hydrocarbon on the product relies on the reaction route and catalyst type.

Interestingly, HDO, with the loading of Ni 3 wt.% produced C_{13} alkanes with a yield up to 44.43% over CPO (palmitic acid and oleic acid). This phenomenon might be due to the strong adsorption of 3 wt.% Ni and give impact in the weakening of the "C–C" bond, which can cause strong catalytic cracking and generate propane molecules as side-products (Chen *et al.*, 2018). Hence, it seemed that the best catalyst was 10% Ni/MIL-96(Al) under the HDO conditions from oxygen-free green diesel compared to 3% Ni/MIL-96(Al) as the optimum catalyst to produce biodiesel.

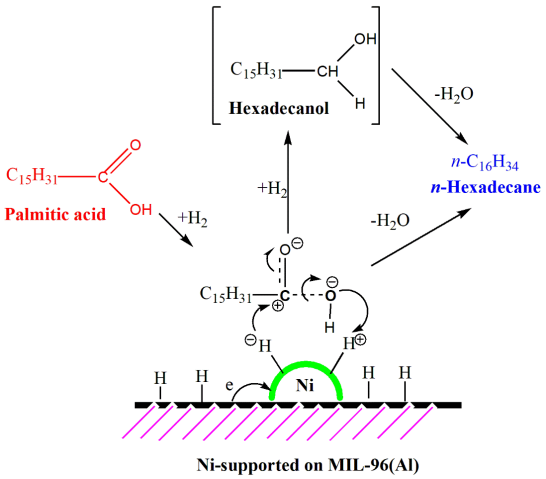

Figure 10 The dominant reaction mechanism proposed for the catalytic reaction using Ni/MIL-96(Al) in the hydrodeoxygenation reaction of CPO

Table 3 Product distribution of the HDO reaction of CPO over MIL-96(Al) and Ni/MIL-96(Al) catalyst

Products Compound	Catalysts			
	MIL-96(Al)	3% Ni/MIL-96(Al)	5% Ni/MIL-96(Al)	10% Ni/MIL-96(Al)
C_7	0	1.12	0	0.5
C_8	0	1.52	0	0.86
C_9	0	3.04	0	1.2
C_{10}	0	0	0.2	0.48
C_{11}	0.43	1.6	0.27	0.59
C_{12}	0.76	3.88	0.47	1.55
C_{13}	1.66	44.43	1.11	2.05
C_{14}	2.25	0	1.2	0
C_{15}	5.83	0	7.01	0
C_{16}	1.04	3.61	0.47	50.09
C_{17}	1.2	0	1.31	0
Alkene	16.25	23.51	12.55	30.5
Oxygenate	69.93	16.19	70.95	9.3
Aromatic	0.65	1.1	4.46	2.88
Green diesel (%)	13.17	53.52	12.04	54.76
Conversion (%)	30.07	83.81	29.05	90.7
Selectivity C_{16} (%)	3.45	4.30	1.61	55.22
% Total product	100	100	100	100

4. Conclusions

MIL-96(Al) was successfully synthesized using a hydrothermal method in a shorter time by adding DMF as an assisting agent. Ni metal loading did not alter or damage the main structure and increased catalytic activity in CPO conversion to biodiesel and green diesel. Optimum catalytic activity for biodiesel production was achieved by 3% Ni/MIL-96(Al) with a yield up to 85.24%. In the case of green diesel production, the material 10% Ni/MIL-96(Al) was found to be the optimum and selective catalyst, with C_{16} (55.22%) as the dominant product. As a preliminary study, this research has shown the potential use of Ni/MIL-96(Al) as a heterogeneous catalyst in biofuel production. However, due to the sensitive nature of MOFs against moisture, pressure, temperature, acid and basic condition, and mechanical treatment, some innovations need to be improved to gain more stable MOFs with high performance in catalytic action. Our group is developing further research in employing highly stable MOF based on tetravalent metal ions such as zirconium, hafnium modified with palladium and nickel metal nanoparticles as catalysts in some organic reaction transformations, including for biofuel production. Composite material between catalytically active MOFs with synthetic and natural zeolites are also currently developed in our group in order to increase stability and catalytic performances of MOFs in biomass conversion as our contribution to the development of sustainable energy solutions.

Acknowledgments

The authors gratefully acknowledge BPDP Sawit (research grant 2017) and Hibah Maintenance Research Group (MRG) PNBP Universitas Sebelas Maret 2017 project number 623/UN.27.21/PP/2017 for supporting this research.

References

Abid, H.R., Rada, Z.H., Shang, J., Wang, S., 2016. Synthesis, characterization, and CO_2 adsorption of three Metal-Organic Frameworks (MOFs): MIL-53, MIL-96, and amino-MIL-53. *Polyhedron*, Volume 120, pp. 103–111

Capuano, L., 2020. International Energy Outlook 2020 (IEO2020). *Centre Strategic and International Studies*

Carmo, A.C., de Souza, L.K.C., da Costa, C.E.F., Longo, E., Zamian, J.R., da Rocha Filho, G.N., 2009. Production of biodiesel by esterification of palmitic acid over Mesoporous Aluminosilicate Al-MCM-41. *Fuel*, Volume 88, pp. 461–468

Čelič, T.B., Grilc, M., Likozar, B., Tušar, N.N., 2015. In situ generation of Ni nanoparticles from metal-organic framework precursors and their use for biomass hydrodeoxygenation. *ChemSusChem*, Volume 8, pp. 1703–1710

Chen, S., Miao, C., Luo, Y., Zhou, G., Xiong, K., Jiao, Z., Zhang, X., 2018. Study of catalytic hydrodeoxygenation performance of Ni catalysts: effects of prepared method. *Renewable Energy*, Volume 115, pp. 1109–1117

Chizallet, C., Lazare, S., Bazer-Bachi, D., Bonnier, F., Lecocq, V., Soyer, E., Quoineaud, A.A., Bats, N., 2010. Catalysis of transesterification by a nonfunctionalized metal-organic framework: acido-basicity at the external surface of ZIF-8 probed by FTIR and ab Initio Calculations. *Journal of the American Chemical Society,* Volume 132(35), pp. 12365–12377

Chughtai, A.H., Ahmad, N., Younus, H.A., Laypkov, A., Verpoort, F., 2015. Metal-Organic frameworks: versatile heterogeneous catalysts for efficient catalytic organic transformations. *Chemical Society Reviews,* Volume 44(19), pp. 6804–6849

Cong, W.J., Nanda, S., Li, H., Fang, Z., Dalai, A.K., Kozinski, J.A., 2021. Metal–organic framework-based functional catalytic materials for biodiesel production: a review. *Green Chem*istry, Volume 23(7), pp. 2595–2618

Fang, R., Dhakshinamoorthy, A., Li, Y., Garcia, H., 2020. Metal organic frameworks for biomass conversion. *Chemical Society Reviews,* Volume 49(11), pp. 3638–3687

Hachemi, I., Kumar, N., Mäki-Arvela, P., Roine, J., Peurla, M., Hemming, J., Salonen, J., Murzin, D.Y. 2017. Sulfur-free Ni catalyst for production of green diesel by hydrodeoxygenation. *Journal of Catalysis*. Volume 347, pp. 205–221.

Hoang, A.T., Le, A.T., 2019. A Review on deposit formation in the injector of diesel engines running on biodiesel. *Energy Sources, Part A: Recovery, Utilization, and Environmental Effects,* Volume 41(5), pp. 584–599

Hoang, A.T., Nižetić, S., Ong, H.C., Tarelko, W., Le, T.H., Chau, M.Q., Nguyen, X.P., 2021a. A review on application of artificial neural network (ANN) for performance and emission characteristics of diesel engine fueled with biodiesel-based fuels. *Sustainable Energy Technologies and Assessments*, Volume 47, p. 101416

Hoang, A.T., Nizetic, S., Ong, H.C., Chong, C.T., Atabani, A.E., Pham, V.V., 2021b. Acid-based lignocellulosic biomass biorefinery for bioenergy production: advantages, application constraints, and perspectives. *Journal of Environmental Management,* Volume 296, p. 113194

Hoang, A.T., Ong, H.C., Fattah, I.M.R., Chong, C.T., Cheng, C.K., Sakthivel, R., Ok, Y.S., 2021c. Progress on the lignocellulosic biomass pyrolysis for biofuel production toward environmental sustainability. *Fuel Processing Technology,* Volume 223, p. 106997

Hoang, A.T., Tabatabaei, M., Aghbashlo, M., Carlucci, A.P., Ölçer, A.I., Le, A.T., Ghassemi, A., 2021. Rice bran oil-based biodiesel as a promising renewable fuel alternative to petrodiesel: a review. *Renewable and Sustainable Energy Reviews,* Volume 135, p. 110204

Huang, Y.B., Liang, J., Wang, X.-S., Cao, R., 2017. Multifunctional metal–organic framework catalysts: synergistic catalysis and tandem reactions. *Chemical Society Reviews,* Volume 46(1), pp. 126–157

Juan-Alcañiz, J., Gielisse, R., Lago, A.B., Ramos-Fernandez, E. V., Serra-Crespo, P., Devic, T., Guillou, N., Serre, C., Kapteijn, F., Gascon, J., 2013. Towards acid MOFS-Catalytic performance of sulfonic acid functionalized architectures. *Catalysis Science & Technology,* Volume 3(9), pp. 2311–2318

Khemthong, P., Yimsukanan, C., Narkkun, T., Srifa, A., Witoon, T., Pongchaiphol, S., Kiatphuengporn, S., Faungnawakij, K., 2021. Advances in catalytic production of value-added biochemicals and biofuels via furfural platform derived lignocellulosic biomass. *Biomass and Bioenergy*, Volume 148, p. 106033

Larasati, I., Winarni, D., Putri, F.R., Hanif, Q.A., Lestari, W.W., 2017. Synthesis of metal-organic frameworks based on Zr^{4+} and Benzene 1,3,5-Tricarboxylate Linker as heterogeneous catalyst in the esterification reaction of palmitic acid. *IOP Conference Series: Materials Science and Engineering,* Volume 214, pp. 1–7

Lestari, W.W., Prajanira, L.B., Putra, R., Purnawan, C., Prihadiyono, F.I., Arrozi, U.S.F., 2021. Green-Synthesized MIL-100(Fe) modified with palladium as a selective catalyst in the hydrogenation of citronellal to citronellol. *Materials Research Express,* Volume 8(4), p. 045504

Liao, Y.T., Matsagar, B.M., Wu, K.C.W., 2018. Metal-Organic Framework (MOF)-derived effective solid catalysts for valorization of lignocellulosic biomass. *ACS Sustainable Chemistry & Engineering,* Volume 6(11), pp. 13628–13643

Liu, D., Liu, Y., Dai, F., Zhao, J., Yang, K., Liu, C., 2015. Size- and morphology-controllable synthesis of MIL-96 (Al) by hydrolysis and coordination modulation of dual aluminium source and ligand systems. *Dalton Trans*actions, Volume 44(37), pp. 16421–16429

Loiseau, T., Lecroq, L., Volkringer, C., Marrot, J., Ferey, G., Haouas, M., Taulelle, F., Bourrelly, S., Llewellyn, P.L., Latroche, M., 2006. MIL-96, a porous aluminum trimesate 3D structure constructed from a hexagonal network of 18-membered rings and μ_3-Oxo-Centered Trinuclear Units. *Journal of the American Chemical Society,* Volume 128(31), pp. 10223–10230

Muharam, Y., Adinda, D.P., 2018. Simulation of hydrotreating of vegetable oil in a slurry bubble column reactor for green diesel production. *International Journal of Technol*ogy, Volume 9(6), pp. 1168–1177

Muharam, Y., Soedarsono, J.A., 2020. Hydrodeoxygenation of vegetable oil in a trickle bed reactor for renewable diesel production. *International Journal of Technol*ogy, Volume 11(7), pp. 1292–1299

Peng, B., Yuan, X., Zhao, C., Lercher, J.A., 2012. Stabilizing catalytic pathways via redundancy: selective reduction of microalgae oil to alkanes. *Journal of the American Chemical Society,* Volume 134(22), pp. 9400–9405

Prihadiyono, F.I., Lestari, W.W., Putra, R., Aqna, A.N.L., Cahyani, I.S., Kadja, G.T.M., 2022. Heterogeneous catalyst based on nickel modified into indonesian natural zeolite in green diesel production from crude palm oil. *International Journal of Technol*ogy, Volume 13, pp. 931–943

Putra, R., Lestari, W.W., Wibowo, F.R., Susanto, B.H., 2018. Fe/Indonesian natural zeolite as hydrodeoxygenation catalyst in green diesel production from palm oil. *Bulletin of Chemical Reaction Engineering & Catalysis,* Volume 13(2), pp. 245–255.

Putra, R., Lestari, W.W., Susanto, B.H., Kadja, G.T.M. 2022. Green diesel rich product (C_{-15}) from the hydro-deoxygenation of refined palm oil over activated NH_4^+-Indonesian natural zeolite. *Energy Sources, Part A: Recovery, Utilization, and Environmental Effects,* Volume 44(3), pp. 7483–7498

Susanto, B.H., Prakasa, M.B., Nasikin, M., Sukirno. 2016. Synthesis of renewable diesel from palm oil and jatropha curcas oil through hydrodeoxygenation using NiMo/ZAL. *International Journal of Technol*ogy, Volume 7(8), pp. 1404–1411

Wan, Y., Chen, C., Xiao, W., Jian, L., Zhang, N., 2013. Ni/MIL-120: an efficient metal-organic framework catalyst for hydrogenation of benzene to cyclohexane. *Microporous Mesoporous Mate*rials, Volume 171, pp. 9–13

Wee, L.H., Janssens, N., Bajpe, S.R., Kirschhock, C.E.A., Martens, J.A., 2011. Heteropolyacid encapsulated in $Cu_3(BTC)_2$ nanocrystals: an effective esterification catalyst. *Catalysis Today*, Volume 171, pp. 275–280

Xamena, F.X.L., Gascon, J., 2013. *Metal organic frameworks as heterogeneous catalysts*. The Royal Society of Chemistry, Cambridge, United Kingdom.

Yang, J., Wang, J., Deng, S., Li, J., 2016. Improved synthesis of trigone trimer cluster metal organic framework MIL-100Al by a later entry of methyl groups. *Chemical Commun*ication, Volume 52(4), pp. 725–728

Yap, M.H., Fow, K.L., Chen, G.Z., 2017. Synthesis and applications of MOF-Derived porous nanostructures. *Green Energy & Environ*ment, Volume 2(3), pp. 218–245

Zhao, H., Chou, L., Song, H., 2011. Exploration of Ni@Zn-MOCP via a wet impregnation strategy as a hydrogenation catalyst. *Reaction Kinetics, Mechanisms and Catalysis,* Volume 104(2), pp. 451–465

Zhao, H., Song, H., Chou, L., 2012. Nickel nanoparticles supported on MOF-5: synthesis and catalytic hydrogenation properties. *Inorganic Chemistry Communications*, Volume 15, pp. 261–265.

Zhao, X., Wei, L., Cheng, S., Julson, J., 2017. Review of heterogeneous catalysts for catalytically upgrading vegetable oils into hydrocarbon biofuels. *Catalysts*, Volume 7, p. 83

Zhen, W., Li, B., Lu, G., Ma, J. 2015. Enhancing catalytic activity and stability for CO_2 methanation on Ni@MOF-5 via controlling active species dispersion. *Chemical Commun*ication, Volume 51(9), pp. 1728–1731

Zuo, H., Liu, Q., Wang, T., Ma, L., Zhang, Qi, Zhang, Qing., 2012. Hydrodeoxygenation of methyl palmitate over supported Ni catalysts for diesel-like fuel production. *Energy and Fuels*, Volume 26, pp. 3747–3755